JOURNAL OF AIRCRAFT
Vol. 48, No. 3, May–June 2011

Material Selection for a Curved C-Spar Based on Cost Optimization

Markus Kaufmann,* Dan Zenkert,† and Malin Åkermo‡
Royal Institute of Technology, SE-10044 Stockholm, Sweden

DOI: 10.2514/1.C000188

A case study for the cost optimization of aircraft structures based on the operating cost as an objective function is presented. The proposed optimization framework contains modules for estimation of the weight, manufacturing cost, nondestructive inspection cost, and structural performance; the latter is enhanced by a kinematic draping model that allows the fiber angles to be simulated more realistically. The case study includes five material systems: aircraft-grade aluminum, two types of resin-transfer molded noncrimp fabric reinforcements, and two types of M21/T800 prepreg. The results are compared in relation to each other, and it is shown that (depending on the estimated fuel burn share of the component) a different material system is favorable when optimizing for low-operating cost.

Nomenclature

C_{man}	=	manufacturing cost, €
$C_{\text{ndt,prod}}$	=	nondestructive testing cost in production, €
$C_{\text{ndt,serv}}$	=	nondestructive testing cost in service, €
C_{tooling}	=	tooling cost, €
DOC	=	direct operating cost, €
N	=	number of regular inspections
p	=	weight penalty, €/kg
W	=	weight, kg
x, $\underline{x}_i$, $\bar{x}_i$	=	design variables, lower and upper limits
α_i	=	correction factors for overheads

I. Introduction

COMPOSITE materials can lower the weight of aircraft structures significantly. By designing 40% of the components in carbon-fiber-reinforced plastics (CFRPs), for example, 1500 kg were saved in the center wing box of the Airbus A380 [1]. The switch to composite materials, however, implies an increased cost for material, processing, and nondestructive testing (NDT). In addition, the design procedures, the quality management, and the production of the components are generally more complex compared with metallic structures. These challenges were identified and described by Gutowski et al. [2], Rais-Rohani and Dean [3], and Soutis [4]. It was concluded that (instead of minimizing the weight) one should take the total life cycle of a component into account when choosing the appropriate material system, manufacturing process, and overall geometry.

Cost/weight optimization frameworks were developed by Kassapoglou [5–7], Park et al. [8], Curran et al. [9,10], and Iqbal and Hansen [11]. One approach to design for cost is to generate a comprehensive amount of design points and to choose the best solution by trading off the cost and weight information. Most of the preceding cost/weight optimization frameworks, however, pursued another strategy that incorporated the cost and weight information into one objective function using weighting factors. Thus, the designer should carefully choose these factors that balance the *cost and weight objectives before performing the optimization*.

Balancing cost and weight objectives is not a simple task. First, one needs to consider the designer's perspective, which could lead to different weighting factors. The amount of fuel burned by an additional kilogram of structural mass, for instance, would lead to a different specific cost per kilogram than the revenue that could be achieved by 1 kg more freight during the lifetime of the aircraft. Again another value per kilogram saved weight could be calculated by the revenue received by an additional passenger during the aircraft's life. In earlier work, it was shown how the optimal design of a skin/stringer structure was dependent on the weight penalty [12]. Subsequently, the methodology was extended by implementation of nondestructive testing costs [13], the suboptimization of parameters for machining [14], and the optimization for the best draping strategy [15].

Here, the foregoing studies were combined and exemplified by means of a case study. In particular, the proposed modules were integrated into one framework, including machining, prepreg/autoclave, and resin-transfer molding (RTM) processes (where applicable), in-production nondestructive testing for composite parts, and different fuel burn shares representing different cost/weight tradeoff functions.

The focus was on the application and comparison of five different material systems for a reference component, i.e., machined aerospace-grade aluminum of type AA7010-T7451, two RTM/noncrimp fabric (NCF) systems of type RTM6/G1157, and two autoclaved M21/T800 prepreg systems. Subsequently, several what-if scenarios were analyzed, examining the effects of changes in labor rate, material cost, or tooling cost.

II. Method

In Kaufmann et al. [12–15], the optimization problem was defined as the minimum of the DOC of an aircraft component, subject to the structural requirements

$$\underline{x}_i < x_i < \bar{x}_i; \qquad i = 1, \ldots, n \tag{1}$$

where DOC is the share of direct operating cost, x_i are design variables, and $\underline{x}_i$ and $\bar{x}_i$ are their lower and upper limits, respectively. The objective function DOC was defined as

$$\text{DOC} = \alpha_1 C_{\text{man}} + \alpha_2 C_{\text{ndt,prod}} + N\alpha_3 C_{\text{ndt,serv}} + pW \tag{2}$$

where C_{man} is the manufacturing cost of the component, $C_{\text{ndt,prod}}$ and $C_{\text{ndt,serv}}$ are costs for nondestructive testing in production and service, p is a weight penalty or a specific fuel burn (in €/kg), and W is the structural weight (in kilograms). The parameters α_i incorporate calibration factors due to depreciation, overhead cost, and other

Received 18 November 2009; revision received 30 September 2010; accepted for publication 18 October 2010.

*Research Assistant, Department of Aeronautical and Vehicle Engineering, Teknikringen 8; kaufmann@kth.se. Student Member, AIAA.
†Professor, Department of Aeronautical and Vehicle Engineering, Teknikringen 8; danz@kth.se.
‡Assistant Professor, Department of Aeronautical and Vehicle Engineering, Teknikringen 8; akermo@kth.se.

adjustments, and N is the number of regular inspections during the lifetime of the component. Throughout this study, the parameters α_i are set equal to one.

The overall optimization framework is shown in Fig. 1. As mentioned previously, it contains several modules that can be activated when necessary. For instance, the NDT module and the composite modeler module are only applied to composite structures, whereas the manufacturing cost, the weight estimation, and the calculation of the structural performance in finite element (FE) analysis are necessary for composite and metallic structures. Note that this framework could easily be enhanced by additional modules. Examples of additional modules are tools for estimation of repair cost or for prediction of the inspection interval.

In this work, Abaqus/CAE was used to model the geometry and to calculate the structural performance and the weight of the component. Given the seamless communication between Abaqus/CAE and the scripting language Python, the latter was used to program all connections and databases of the optimization framework. The manufacturing cost was modeled by means of the commercial cost estimation package SEER for Manufacturing (SEER-MFG), developed by Galorath, Inc. This software package provided the necessary levels of detail, which are needed to forward sensitive finite difference information to the solver. In principle, the proposed methodology was independent of the choice of the cost modeling tool. SEER-MFG was chosen for convenience and the fact that it was widely accepted by the aircraft industry.

A. Extended Nondestructive Testing Module

Apart from the commercially available cost estimation and FE models, a module for the estimation of nondestructive testing cost was developed and implemented [13]. This module did not only affect the cost but also the material properties of the structural model by variation of the permissible flaw size of a laminate and estimation of the through-the-thickness porosity. Depending on the input parameters, such as width, length, thickness, and permissible flaw size of the panel, the necessary scan pitch of an ultrasonic scan (one transducer, no phased array) was estimated based on a given probability of detection (POD). For example, a larger permissible flaw size resulted in a wider scan pitch (dk in Fig. 1) while maintaining a certain POD.

Similarly, it lowered the design strength of the material, as larger flaws could remain undetected during the quality control of the component. Based on the work on notched specimens by Soutis et al. [16], the strength degradation of a flaw size other than 6 mm was modeled by the law,

$$\hat{\sigma}_f(f) = \hat{\sigma}_0[1 - A(f - 6)] \tag{3}$$

where $\hat{\sigma}_f$ is the updated material strength due to flaws, $\hat{\sigma}_0$ is the material strength at a standard flaw size of 6 mm, A is a material-specific strength degradation constant, and f is the permissible flaw size.

The strength degradation due to porosity was defined as a function of the thickness. Similar to the work published by Uhl et al. [17] and Lee and Soutis [18,19], the calculation of the updated material strength due to porosity was done according to the relation,

$$\hat{\sigma}_p(t) = \hat{\sigma}_0 e^{B(t-t_0)} \tag{4}$$

where $\hat{\sigma}_0$ is the material strength of a laminate with thickness t_0, t is the thickness of the laminate, and B is a material parameter. The structural model was then updated using the minimum of the calculated material strengths; that is,

$$\hat{\sigma} = \min(\hat{\sigma}_f, \hat{\sigma}_p) \tag{5}$$

The cost of NDT was calculated using a feature-based kinematic cost model. Depending on the type of feature and the previously updated scan pitch, a one-dimensional or two-dimensional scan pattern was simulated, and the scan time estimated. Features included thin flat laminates with access from both sides, thin flat laminates with access from one side, thick flat laminates with access from both sides, thick flat laminates with access from one side, radii, or adhesive bonds. Each of these features required input data in the form of the length, the width, the thickness, and (in case of radii) the radius. The feature definition consisted of the scanning technique and equipment, a complexity index coupled to the type of feature, the educational level of the operator, and (associated with the latter) a labor rate. During the setup of the cost model, the corresponding features could be selected. Throughout the optimization, the cost to scan a feature was calculated, and the estimates fed back to the global cost model [13].

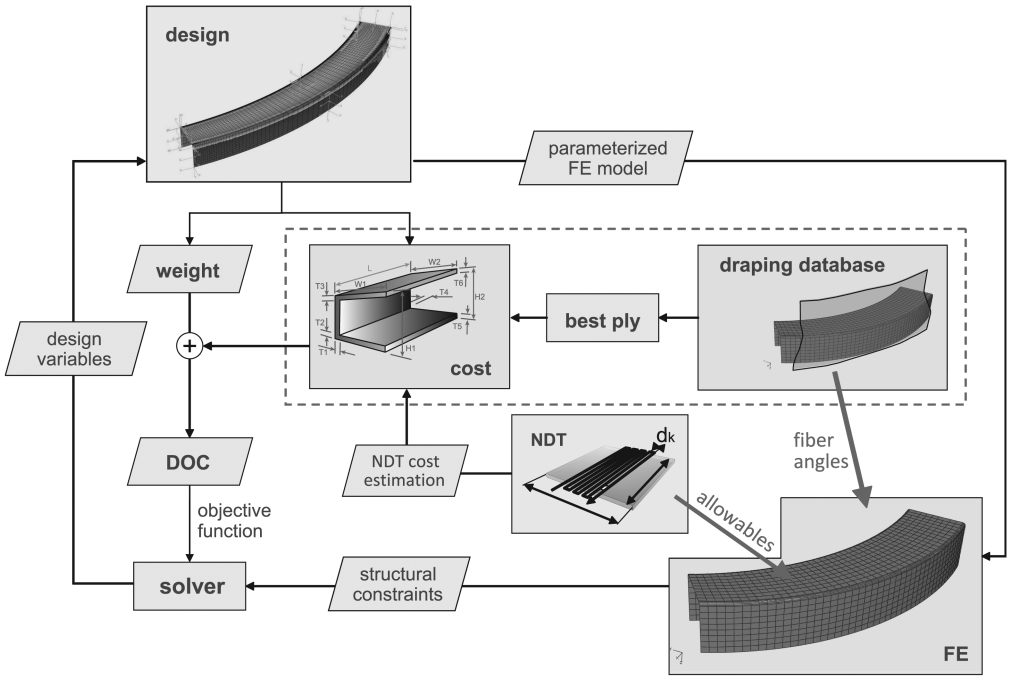

Fig. 1 Optimization framework.

B. Extended Manufacturing Module

The results shown in Kaufmann et al. [12,13] indicated that the initial settings of the machining and composite layup parameters did not always match the expert knowledge of the manufacturing engineer. In particular, the choice of the cutter (in the case of aluminum) or the draping strategy (in case of CFRP prepreg) could have an influence on the final manufacturing cost. For the optimization of machined components, a routine for the suboptimization of machining parameters was developed in order to guarantee the lowest possible manufacturing cost for a given geometrical design [14].

For the case of composites, the draping of the plies was modeled using the kinematic draping simulation tool Composite Modeler. The advantages of Composite Modeler were the seamless integration into Abaqus/CAE, the parametrization with Python, and the short calculation time due to the kinematic draping code based on the pin-jointed net algorithm [20,21]. The outputs from this model were the fiber angle distribution and an unfolded outline of the draped ply: the so-called flat pattern. The flat pattern was postprocessed in order to calculate the length of the ultrasonic cut, the ply area, and the material consumption (the area of a surrounding rectangle including ply area plus waste). Thus, the draping module affected both the cost model (material consumption, ultrasonic cutting, and number of plies) and the structural model (fiber angle after draping and number of plies). As a consequence, the impact of a draping strategy could be examined in terms of cost and weight; that is, the seed point (location of initial contact between the ply stack and the next layer) and the reference angle (angle between the new layer's 1-axis and a reference coordinate system). For the nomenclature, see Fig. 2.

It would be too time consuming to optimize the seed point and reference angle during the optimization of the geometry, since a full FE calculation is needed for the evaluation of each design strategy. Instead, a draping database *was generated before the optimization took place*. Thus, a series of different seed point/reference angle combinations was examined and stored in terms of material consumption, ultrasonic cutting, and resulting fiber angles. During the optimization, sets of best plies were chosen according to minimum material consumption or minimum fiber angle deviation rules. Detailed information can be found in Kaufmann et al. [15].

The optimization framework was implemented by means of Abaqus/CAE, Composite Modeler, SEER-MFG, and the scripting language Python. Using material data provided by Saab Aerostructures and Airbus, an extensive case study was performed. The result of this case study is explained in the following section.

III. Case Study

For the case study, a double-curved C-spar (a representative fuselage component of a next-generation twin-aisle airliner) was chosen, as depicted in Fig. 3. The loading conditions and constraints are arbitrary for the methodology and therefore much simplified for the sake of reduced computation time. As illustrated, the spar contained simply supported boundary conditions at the edges of the inner flange, and it was loaded by a uniformly distributed pressure at the outer flange. Other constraints comprehended the maximum displacement of the outer flange and the material-specific strain and stress limits. A shell model with 6480 linear quadrilateral elements of type S4R was used for the structural model. Five material systems were chosen for the optimization and comparison: machined aluminum, two RTM6/NCF reinforcements, an M21/T800 plain weave (PW) prepreg, and an M21/T800 unidirectional (UD) prepreg.

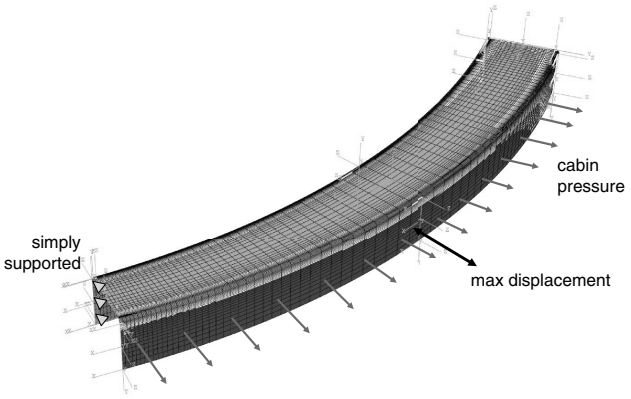

Fig. 3 Double-curved C-spar.

As the baseline, the C-spar was cost-optimized using the objective function,

$$\mathrm{DOC} = C_{\mathrm{man}} + C_{\mathrm{ndt,prod}} + pW \tag{6}$$

where the weight penalty p was varied between zero and ∞. A weight penalty of $p = 0$ corresponded to pure cost optimization, as the influence of the weight was zero. At the other extreme, $p = \infty$ corresponded to pure weight optimization. The effects of varying p were shown earlier by means of a stiffened skin/stringer panel [12,13]. In these articles, reasonable weight penalties were estimated at €1500–2000/kg. A change of the optimizer's viewpoint from fuel saving to increased revenue, however, would lead to a much higher weight penalty of approximately €30,000/kg.

Unlike the case of a stiffened panel, we expected the cost- and weight-optimal solutions of the composite spars to be very similar, since both the RTM and the prepreg/autoclave were additive processes. *Thus, the comparison of the different* material systems and the location of the break-even points were in the focus of this study. Only recurrent costs were considered first. Nonrecurrent costs (such as the tooling cost) were included in a second step. In Table 1, the common parameters of the case study are given. Note that these values do not necessarily correspond to values used at Saab and Airbus due to reasons of confidentiality. In particular, the otherwise arbitrary production quantity should reflect a mature manufacturing process in combination with reasonable depreciation costs for tooling. The direct labor rate is fully built up; that is, it contains the cost for manual labor, machines and equipment, and overhead.

A. Machined Aluminum AA7010-T7451

The aluminum spar was high-speed machined from a precut bar stock. Two machining operations (rough and finish) were modeled. Unlike the case of composites, no nondestructive testing cost was included apart from a dimension check, the latter accounting for 8% of the labor cost. The labor time underwent an adjustment due to learning curves in order to reflect the time needed when a quantity of 100 components was produced.

Two cases were examined: first, the case with one thickness variable over the total spar; thereafter, the case where three optimization variables were used (one for the inner flange, one for the spar

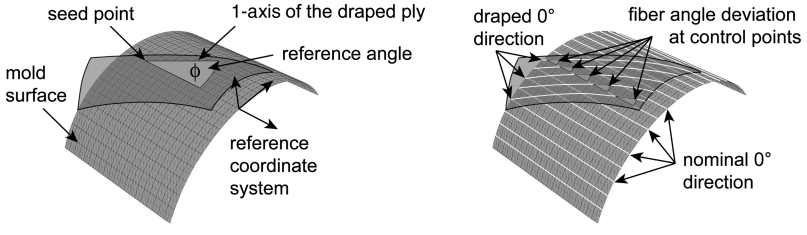

Fig. 2 Definitions of seed point, reference coordinate system, reference angle, nominal fiber direction, draped fiber direction, and fiber angle deviation.

Table 1 Common properties for the baseline scenario

Property	Value
Production quantity	100
Direct labor rate, €/h	150
Overall length, mm	1180
Web width, mm	120–150
Web height, mm	100
Uniform pressure, MPa	0.14

Table 2 Properties for AA7010-T7451

Property	Value
Material cost, €/kg	7.5
Density (ρ), kg/m^3	2700
Young's modulus (E), GPa	71.0
Poisson's ratio (ν)	0.30
Failure strength ($\hat{\sigma}$), MPa	490

web, and one for the outer flange). Two constraints were active: a von Mises criterion and a maximum displacement criterion. Aluminum-specific properties are given in Table 2.

B. RTM6/G1157

The cost model for the RTM/NCF material system included the following parts: costs for material, consumables, tool cleaning, material placement, tool closing, curing, and finishing. The nondestructive testing cost included five parts: costs for the inner flange, the inner radius, the web, the outer radius, and the outer flange. The laminates were assumed to be scanned using an automated pulse-echo squirter, as access was provided from one side only. The two radii were scanned using a manual flaw detector. First, only UD NCF fabrics were considered. Then, the spar was modeled using a longitudinal/transverse (LT) fabric for the $0/90°$ plies and a double bias (DB) fabric for the $\pm 45°$ plies in order to save touch labor and waste. Thus, the tradeoff between the cost for cutting and stacking and the design flexibility when switching from UD to biaxial fabrics could be examined. Figure 4 shows an overview of these fabrics.

In the case of RTM, the parameters A and B [Eqs. (3) and (4)] were set to -0.032 and 0.0079, respectively. Note that an RTM component has slightly more porosity than a similar prepreg/autoclave component, which is reflected in the choice of these parameters. Other properties for the RTM/NCF material system are given in Table 3.

C. M21/T800 Prepreg

A PW and a UD M21/T800 material system were examined. The cost model was implemented similarly to the RTM/NCF cost model. The main difference was the rather time-consuming debulking phase during the placement of the material. The NDT cost model also involved the same features and inspection techniques as for the RTM/NCF case. The strength degradation due to porosity and flaw sizes was governed by the parameters $A = -0.028$ and $B = 0.0079$. Other properties are given in Table 4.

Apart from the optimization with varying weight penalty, a series of what-if scenarios was investigated. These scenarios included the examination of the effects of nonrecurrent costs, different labor rates, decreasing material prices, and changes in production quantity. Based on these scenarios, the sensitivity of the break-even points for aluminum, NCF, and prepregs could be discussed.

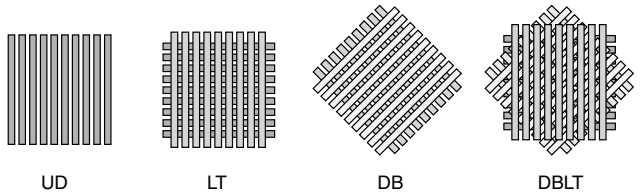

Fig. 4 Uniaxial, biaxial, and quadraxial NCF reinforcements. Only UD, LT, and DB fabrics were used in this study.

Table 3 Properties for RTM6/G1157[a]

Property	Variable	UD	LT
Material cost NCF, €/kg		60	60
Material cost RTM6, €/kg		90	90
Density, kg/m^3	ρ	1500	1500
Ply width, m	b	1.3	1.3
Young's moduli, GPa	E_1	136	70
	E_2	9.4	70
Shear moduli, GPa	G_{12}	5.4	5.4
	G_{13}	3.1	3.1
	G_{23}	3.1	3.1
Poisson's ratio	ν_{12}	0.30	0.039
Strength, MPa	$\hat{\sigma}_{1t}$	1970	523
	$\hat{\sigma}_{1c}$	990	529
	$\hat{\sigma}_{2t}$	67	523
	$\hat{\sigma}_{2c}$	240	529
	$\hat{\sigma}_{12}$	62	62
Shear locking angle, °	θ	60	30

[a]Values are given for the UD and for the LT reinforcement; the latter were estimated using laminate theory.

Table 4 Properties for M21/T800[a]

Property		PW	UD
Material cost, €/kg		167	81
Density, kg/m^3	ρ	1550	1550
Ply width, m	b	1.2	1.2
Young's moduli, GPa	E_1	75	142
	E_2	75	7.8
Shear moduli, GPa	G_{12}	4.2	5.4
	G_{13}	4.2	3.1
	G_{23}	4.2	3.1
Poisson's ratio	ν_{12}	0.037	0.30
Strength	$\hat{\varepsilon}_{1t}$	0.005	0.005
	$\hat{\varepsilon}_{1c}$	−0.004	−0.004
Shear locking angle, °	θ	30	10

[a]Values are given for PW and UD prepreg.

IV. Results and Discussion

Figure 5 and Tables 5 and 6 summarize the results of the baseline scenario for aluminum and composites. Results depicted with ▼ refer to cost-optimized solutions. and △ refers to a weight-optimized solution. In the following, some of these results are discussed.

No significant changes in cost could be observed when changing from one to three variables in the case of the aluminum spar. The saving in weight, however, was 0.6 kg (or 5.8%) if optimized with three variables, referred to as ALU △ in Fig. 5. Feasible solutions could only be obtained for weight penalties $p \geq 0$, as the purely cost-optimized solution (with $p = 0$) tended toward minimum machining time and resulted in an unmachined raw stock of initial size. The cost-optimized results, ALU ▼, were therefore omitted.

For the RTM (UD) spar, a distinct change in layup, cost, and weight could be seen when changing from a low-cost to a low-weight design configuration. In this case, the difference in manufacturing cost was €549, or 33%, due to the better material usation when optimizing for cost. Despite the lower C_{man} of the low-cost configuration, the cost for nondestructive testing C_{ndt} increased as a consequence of the thicker structure. Accordingly, the cost-optimized solution was 1 kg, or 14%, heavier than the weight-optimized solution. Here, the effect of the two opposing objectives, cost and weight, can be seen. In reality, one would obtain the best compromise between the two extremes, ▼ and △, by assigning an intermediate weight penalty p to the objective function (6). For

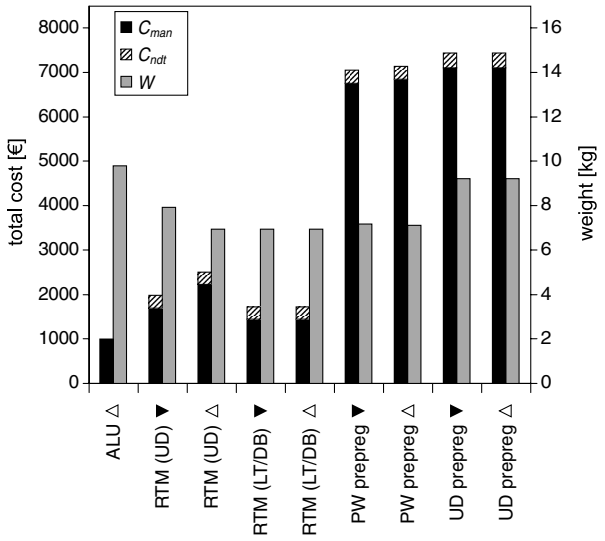

Fig. 5 Estimations of weight W, manufacturing cost C_{man}, and cost for nondestructive testing C_{ndt}. Results marked with △ were weight optimized (p large), and entries marked with ▼ were cost optimized (p small).

certain types of components, the design solution is very sensitive to the choice of the weight penalty, as shown for stiffened panels in Kaufmann et al. [12,13]. For other types of components (such as the curved C-spar presented herein), the design solution is less sensitive and the design space more of binary nature. In this case, the low-cost and the low-weight solutions are separated by a distinct break-even point, as shown later in more detail.

No big differences in cost and weight for the two objectives can be seen in case of the RTM (LT/DB) material system. As mentioned before, LT material was used for 0° plies, and DB material was used for the ±45° plies. By choosing two different types of reinforcements, scrap (and thus the material consumption) could be reduced, compared with the UD material of the foregoing case. For this type of component, a smart selection of the reinforcement type would lead to the very same design solution for a wide range of weight penalties p, as no savings in raw material was possible. Thus, design solutions of the opposing cost and weight-optimized RTM (LT/DB) designs were very similar.

A rise in manufacturing cost can be seen when changing from RTM to autoclave processes. The weight-minimized PW prepreg provided a reasonable structural performance with the drawback of the high manufacturing cost, compared with the aluminum and the RTM solutions. Note the change in fiber layup, cost, and weight when switching from a cost-optimized (▼) to a weight-optimized (△) design. Both solutions were ±45° dominated, as these plies provided higher structural performance for the given load case. The low-cost design, however, resulted in slightly thicker 0/90° layers, as this generated less scrap, thus leading to savings in material cost. Translated to composite design in general, one should carefully examine the material consumption of a particular design solution with respect to scrap. If neglected, one might overlook a more cost-effective layup with only small increases in weight.

Table 5 Results of the aluminum (ALU)

Case	Inner flange, mm	Web, mm	Outer flange, mm
ALU (1 variable)[a]	9.9	9.9	9.9
ALU (3 variables)[a]	12.8	8.0	8.0

[a]Weight optimized (p large).

Table 6 Results of the RTM (UD and LT/DB), the PW prepreg, and the UD prepreg systems

Case	0°, mm	90°, mm	±45°, mm
RTM (UD)[a]	1.61	4.97	0.15
RTM (UD)[b]	0.24	0.88	2.44
RTM (LT/DB)[a]	0.60	——	5.39
RTM (LT/DB)[b]	0.70	——	5.30
PW prepreg[a]	2.00	——	4.00
PW prepreg[b]	1.59	——	4.34
UD prepreg[a]	0.25	0.81	3.32
UD prepreg[b]	0.25	0.72	3.36

[a]Cost optimized (p small).
[b]Weight optimized (p large).

The design with UD prepreg was highly constrained by the shear locking angle of 10°, which rendered most of the draping strategies infeasible. Only a reduced set of seed points and reference angles was available for this material system, implicating high fiber angle deviations and high scrap ratios. Thus, the UD prepreg spar was heavier than the PW spar and had a higher manufacturing cost as a result of the extensive time needed for layup and debulking. In reality, one would introduce a number of splits in the prepreg in order to minimize the effect of fiber angle deviations and to enhance drapability. These splits were not part of the model and therefore distorted the quality of the results significantly. In more recent versions of Composite Modeler, splits can be introduced. Thus, the optimization of the fiber angle deviation and the material shear with respect to the position and length of the split could be integrated in the future.

Comparing cost and weight data across different material systems (Fig. 5), one can observe that the aluminum spar provided the most cost-efficient solution, whereas the weight-minimized RTM solution was best in terms of structural performance. The NCF fabric's good drapability provided a large design space in terms of draping strategies, which led to an overall good cost/weight performance. These trends are also represented in the designs of next-generation twin-aisle airliners, where this shift from machined aluminum to autoclaved prepreg and to RTM processes can be observed. Examples for RTM parts are fittings, window frames, fuselage frames, aileron spars, engine ducts and blades, and components of the landing gear.

The prepreg systems were not as cost efficient as the RTM systems. The high cost level was a consequence of the much higher touch labor during the material placement and debulking phase of the prepreg system. The estimated material layup and tool closing time for the cost-optimized RTM (LT/DB) system, for example, was 179 min., whereas the same processes in the case of PW prepreg accumulated to a total of 1097 min. This time-consuming process could be replaced by the use of an automated tape layer or an automated fiber placement machine that enables material placement without the need for debulking. The consequence is a much more competitive manufacturing process for prepreg systems. Not all geometries can be laid up by these techniques though. Examples where autoclaved prepreg systems can exceed are straight, flat members, such as wing skins and the center wing box (using automated tape layers) or fuselage barrels (using automated fiber placement machines).

Even though the NDT cost was roughly the same, the relative impact on the total cost was much higher for the RTM system (10.8–15.7%) than for the prepreg system (4.0–4.4%). Apparently, there is a need for more cost-efficient techniques than single-probe ultrasonic scanning, and the use of phased-array scanners can lower this cost, as a bigger area can be covered by a single sweep.

Using the DOC as the objective function provided a tool to combine cost and weight objectives by applying a weight penalty p. The quantification of this weight penalty was not trivial, since different viewpoints could be adopted. Instead, the effect of varying p, literally changing the viewpoint from pure cost to pure weight optimization, was examined. Figure 6 shows the results of the variation of p from zero to ∞.

At the far left, one can compare the production cost of the spar, since the weight penalty, and thus the impact of the weight objective, was zero. As shown earlier in Fig. 5, the lowest manufacturing cost was achieved for the aluminum spar, followed by the RTM/NCF, the

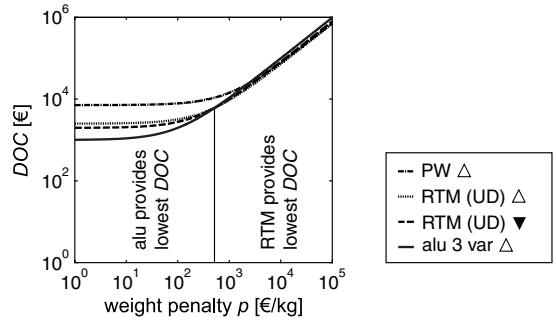

Fig. 6 DOC versus weight penalty p for the baseline. For the sake of simplicity, only the results of the aluminum, the RTM, and the PW materials are shown. Results marked with △ were weight optimized (p large), and entries marked with ▼ were cost optimized (p small).

PW, and the UD prepreg systems. As p increased, the impact of the weight on the objective function increased. Thus, a break-even point between aluminum and RTM/NCF was reached at €528/kg. When increasing p further, the RTM system remained favorable, as both the UD and the PW prepreg systems suffered from higher weight.

A. What-If Scenarios

The cost-optimization framework allowed for the examination of the sensitivity of variations in labor rates, material costs, and production quantity. First, the effect of the nonrecurrent cost was examined. For the baseline scenario, no tooling cost was included in the cost model. Now, the cost of a double-sided mold was calculated according to SEER-MFG standards ($C_{\text{tooling}} = €60,000$) and €600 were added to each component during the postprocessing of the results. In Fig. 7, the DOC versus the weight penalty p for aluminum and cost-minimized RTM are shown in a log–log graph. As can be seen, the RTM/NCF design including tooling costs suffered from a slightly increased total cost compared with the baseline. The result was a shifted point of break-even between aluminum and RTM (UD), now located at $p = €740/\text{kg}$.

Second, the cost for the raw material was varied between −33 and +100%, reflecting scenarios for material shortages or abundances. The result is shown in the range plot of Fig. 8. As can be seen, the location of the break-even point varied between the extremes: 1) high aluminum, low resin and binder cost break even at €146.4; and 2) low aluminum, high resin and binder cost break even at €928.3.

Likewise, the effects of different labor rates were examined. Thus, the labor rate of €150/kg was lowered to €50/kg in order to reflect the conditions of a low-wage country. In this case, the total cost of the aluminum spar was €957, which was a reduction of 4.2%. In the case of weight-optimized RTM (UD), the change of the labor rate would lead to manufacturing and NDT costs of €1773 and €150.1, respectively, which was a total reduction of 23.2%. For the weight-optimized UD prepreg, this difference was even bigger. There, the manufacturing and NDT costs decreased to €3888 and €171.7,

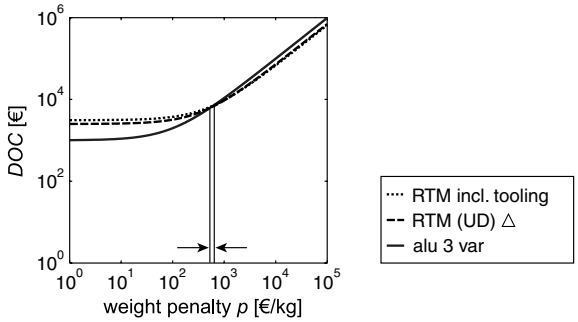

Fig. 7 DOC versus weight penalty for aluminum and RTM (UD) if the cost of a double-sided mold was included. Note the shifted break-even point from €528/kg to €740/kg. The values for both RTM spars refer to weight-optimized solutions (p large).

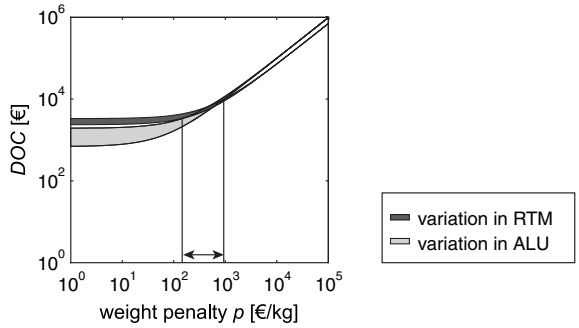

Fig. 8 DOC versus weight penalty with varying costs for raw material. Shown are the ranges for aluminum and RTM (UD).

respectively, which was a total reduction of 45.4%. The higher potential of cost savings for the composite spar was explained by its higher share of touch labor. In particular, the production of a prepreg spar in a low-wage country could cut the total cost by almost 50%.

No big change in manufacturing costs was observed when the production quantity was increased from 100 to 1000 spars. The costs for both aluminum and RTM were modeled using fairly established manufacturing processes with a large number of preproduction units and a high experience in SEER-MFG terminology. Thus, the effect of the additional learning was less than 1% for the increased production quantity. Note, however, that the nonrecurring costs (such as molds) are divided by the number of produced components. Therefore, the tooling costs would decrease from €600 to €60 per unit when changing from 100 to 1000 spars. The total cost, including nonrecurrent cost ($C_{\text{man}} + C_{\text{ndt}} + C_{\text{tooling}}$), of the weight-optimized RTM (UD) spar, for instance, would decrease from €3105 to €2563.

B. Variable Laminate Quality

The standard flaw size in the foregoing calculations was 6 mm, which resulted in a scan pitch of approximately 2 mm (maintaining a POD of 95%). Only the stiffness, but not the maximum stress criterion, was active for the weight-optimized RTM part. Therefore, one could imagine lowering the design strength without compromising the structural performance.

As described in Sec. II.A, the NDT module allowed the variation of the permissible flaw size, which was increased to 12 and 20 mm (Table 7). The scan pitch was then adjusted in order to maintain a POD of 95%. As a consequence, the allowables were lowered to reflect the inferior level of guaranteed laminate quality.

No change in the design was seen when increasing the flaw size to 12 mm. Again, the design was constrained by an active stiffness criterion that is unaffected by the NDT module. The inspection cost, however, decreased from €270 to €162 due to the wider scan pitch, which shortened the total scan time. Increasing the permissible flaw size to 20 mm lowered the C_{ndt} even further. As the design strength of the material was coupled to the permissible flaw size, the strength criterion became active in this case, and the spar design experienced a slight increase in weight. At the same time, the manufacturing cost decreased from €2235 to €2213 due to the reduced number of material-extensive ±45° layers.

Finally, the permissible flaw size f was used as a variable in order to cost optimize the spar. The cost-optimal flaw size was found at 10.5 mm, lowering the C_{ndt} from €291 to €190. Thus, the total cost decreased by 4.7%. In this case, both the stiffness and the strength criteria were active in the optimized configuration. Changing the level of guaranteed laminate quality could save some cost for nondestructive testing at little or no weight increase. Much material testing would be necessary, however, in order to convince the authorities and the aircraft manufacturers of the sustained safety of the aircraft.

None of these results should be generalized. The use of different input data (such as labor rates, costs for raw material, and process parameters) could lead to deviations in the results for cost, weight, and break-even points.

Table 7 RTM with different laminate qualities[a]

Case	0°, mm	90°, mm	±45°, mm	Weight, kg	C_{man}, €	C_{ndt}, €
RTM UD (6 mm flaw)[b]	0.24	0.88	2.44	6.95	2235	270
12 mm flaw[b]	0.24	0.88	2.44	6.95	2235	162
20 mm flaw[b]	0.19	1.12	2.35	6.97	2213	118
RTM UD (6 mm flaw)[c]	1.61	4.97	0.15	7.92	1686	291
Cost-optimal flaw size[c]	2.00	4.61	0.13	7.94	1694	190

[a]The cost-optimal laminate quality was found at a flaw size of 10.5 mm.
[b]The variation of the flaw size was done for the weight-minimized RTM (UD) spar.
[c]The optimization of the flaw size was done for the cost-optimized RTM (UD) spar.

First, it is necessary to challenge the assumptions and the validity of the models. For instance, current trends lead toward phased-array ultrasonic scanners for the in-production inspection. Such scanners use a fixed scan pitch that cannot be altered as a design variable. Thus, the optimization of the quality level would not lead to a change in scan cost as proposed in this work. The POD, however, would vary, and one could imagine the introduction of a cost penalty as a function of the POD.

For the calculation of the material consumption, the flat pattern of the draping simulation, as well as the scrap around it, was included. In reality, one could use a nesting algorithm in order to minimize the scrap ratio. Hence, the material consumption used throughout this paper was regarded as an upper bound. Enhancing the framework by the implementation of such a nesting algorithm would be interesting.

V. Conclusions

An integrated cost/weight optimization framework was proposed and exemplified by means of a case study. The selection of the material system should be based on the cost-saving potential during manufacturing and operation, since neither design for lowest cost nor design for lowest weight necessarily reflect the true objectives of the designer.

Using a simplified form of DOC, it was shown how the choice of the material system depended on the applied weight penalty. The prepreg material suffered from significant drawbacks when it came to cost efficiency. Both the PW and the UD prepreg had much higher touch labor in combination with very little or no weight benefits: the latter mainly due to the reduced drapability of the UD system. It can, however, be assumed that UD prepregs perform better for less curved components where little or no drapability is needed.

For low weight penalties, the aluminum spar provided the cost-optimal solution. For high weight penalties, the weight-optimized UD and biaxial NCFs provided the best structural performance. The total costs of these systems, however, was very different: one would choose a biaxial fabric if not only weight was regarded as the objective.

In a parameter study, the effects of tooling costs, variations in costs for raw materials, changes in labor rates, and a higher production quantity were examined. They were focused on the behavior of the break-even point between aluminum and RTM UD fabric. Depending on the choice of the weight penalty during the actual design of the spar, another material system would be selected.

Finally, an extended nondestructive testing module was used to simulate and vary the permissible flaw size during the optimization. It was shown that some cost saving was possible if larger flaws were permitted, since the costs for nondestructive testing could be lowered. The framework also allowed for the optimization of the flaw size for minimum production cost, which resulted in a reduction of 4.7%.

Acknowledgments

This work is part of the European Framework Program 6, project "Advanced Low Cost Aircraft Structures" (ALCAS, AIP4-CT-2003-516092), and the Swedish National Aeronautics Research Programme 4, project "Kostnadseffektiva Kompositstrukturer" (KEKS). Special thanks go to Simulayt, Inc., for the use of Composite Modeler, to Alfgam, AB, for the use of Xopt, and to Galorath International, for the use of SEER for Manufacturing. Finally, the collaboration with Tonny Nyman and Per Hallander at Saab Aerostructures is thankfully acknowledged.

References

[1] Marsh, G., "Composites Lift Off in Primary Aerostructures," *Reinforced Plastics*, Vol. 48, No. 4, April 2004, pp. 22–27. doi:10.1016/S0034-3617(04)00193-6

[2] Gutowski, T., Henderson, R., and Shipp, C., "Manufacturing Costs for Advanced Composites Aerospace Parts," *SAMPE Journal*, Vol. 27, No. 3, 1991, pp. 37–43.

[3] Rais-Rohani, M., and Dean, E. B., "Toward Manufacturing and Cost Considerations in Multidisciplinary Aircraft Design," Proceedings of 37th AIAA/ASME/ASCE/AHS/ASC Structures, Dynamics and Materials Conference and Exhibit, Salt Lake City, UT, AIAA Paper 1996-1620, April 1996.

[4] Soutis, C., "Fibre Reinforced Composites in Aircraft Construction," *Progress in Aerospace Sciences*, Vol. 41, No. 2, 2005, pp. 143–151. doi:10.1016/j.paerosci.2005.02.004

[5] Kassapoglou, C., "Simultaneous Cost and Weight Minimization of Composite Stiffened Panels Under Compression and Shear," *Composites Part A: Applied Science and Manufacturing*, Vol. 28, No. 5, 1997, pp. 419–435. doi:10.1016/S1359-835X(96)00141-8

[6] Kassapoglou, C., "Minimum Cost and Weight Design of Fuselage Frames. Part A: Design Constraints and Manufacturing Process Characteristics," *Composites Part A: Applied Science and Manufacturing*, Vol. 30, No. 7, 1999, pp. 887–894. doi:10.1016/S1359-835X(98)00190-0

[7] Kassapoglou, C., "Minimum Cost and Weight Design of Fuselage Frames. Part B: Cost Considerations, Optimization, and Results," *Composites Part A: Applied Science and Manufacturing*, Vol. 30, No. 7, 1999, pp. 895–904. doi:10.1016/S1359-835X(98)00191-2

[8] Park, C. H., Lee, W. I., Han, W. S., and Vautrin, A., "Simultaneous Optimization of Composite Structures Considering Mechanical Performance and Manufacturing Cost," *Composite Structures*, Vol. 65, No. 1, 2004, pp. 117–127. doi:10.1016/j.compstruct.2003.10.010

[9] Curran, R., Raghunathan, S., and Price, M., "Review of Aerospace Engineering Cost Modelling: The Genetic Causal Approach," *Progress in Aerospace Sciences*, Vol. 40, No. 8, 2004, pp. 487–534. doi:10.1016/j.paerosci.2004.10.001

[10] Curran, R., Rothwell, A., and Castagne, S., "Numerical Method for Cost-Weight Optimization of Stringer-Skin Panels," *Journal of Aircraft*, Vol. 43, No. 1, 2006, pp. 264–274. doi:10.2514/1.13225; also AIAA Paper 0021-8669.

[11] Iqbal, A., and Hansen, J. S., "Cost-Based, Integrated Design Optimization," *Structural and Multidisciplinary Optimization*, Vol. 32, No. 6, 2006, pp. 447–461. doi:10.1007/s00158-006-0026-x

[12] Kaufmann, M., Zenkert, D., and Wennhage, P., "Integrated Cost/Weight Optimization of Aircraft Structures," *Structural and Multidisciplinary Optimization*, Vol. 41, No. 2, 2010, pp. 325–334. doi:10.1007/s00158-009-0413-1

[13] Kaufmann, M., Zenkert, D., and Mattei, C., "Cost Optimization of Composite Aircraft Structures Including Variable Laminate Qualities," *Composites Science and Technology*, Vol. 68, No. 13, 2008, pp. 2748–2754. doi:10.1016/j.compscitech.2008.05.024

[14] Kaufmann, M., Czumanski, T., and Zenkert, D., "Manufacturing Process Adaptation for the Integrated Cost/Weight Optimisation of Aircraft Structures," *Plastics, Rubber and Composite*, Vol. 38, No. 2,

2009, pp. 162–166.
doi:10.1179/174328909X387793

[15] Kaufmann, M., Zenkert, D., and Åkermo, M., "Cost/Weight Optimization of Composite Prepreg Structures for Best Draping Strategy," *Composites Part A: Applied Science and Manufacturing*, Vol. 41, No. 4, 2010, pp. 464–472.
doi:10.1016/j.compositesa.2009.11.012

[16] Soutis, C., Smith, F. C., and Matthews, F. L., "Predicting the Compressive Engineering Performance of Carbon Fibre-Reinforced Plastics," *Composites Part A: Applied Science and Manufacturing*, Vol. 31, No. 6, 2000, pp. 531–536.
doi:10.1016/S1359-835X(99)00103-7

[17] Uhl, K. M., Lucht, B., Jeong, H., and Hsu, D. K., "Mechanical Strength Degradation of Graphite Fiber Reinforced Thermoset Composites Due To Porosity," *Review of Progress In Quantitative Nondestructive Evaluation*, Vol. 7B, 1988, pp. 1075–1082.

[18] Lee, J., and Soutis, C., "Thickness Effect on the Compressive Strength of T800/924C Carbon Fibre-Epoxy Laminates," *Composites Part A: Applied Science and Manufacturing*, Vol. 36, No. 2, 2005, pp. 213–227.
doi:10.1016/j.compositesa.2004.06.010

[19] Lee, J., and Soutis, C., "A Study on the Compressive Strength of Thick Carbon Fibre-Epoxy Laminates," *Composites Science and Technology*, Vol. 67, No. 10, 2007, pp. 2015–2026.
doi:10.1016/j.compscitech.2006.12.001

[20] Mack, C., and Taylor, H. M., "The Fitting of Woven Cloth To Surfaces," *Journal of the Textile Institute*, Vol. 47, Vol. 2, 1956, pp. 477–488.

[21] Wang, J., Paton, R., and Page, J. R., "Draping of Woven Fabric Preforms and Prepregs for Production of Polymer Composite Components," *Composites Part A: Applied Science and Manufacturing*, Vol. 30, No. 6, 1999, pp. 757–765.
doi:10.1016/S1359-835X(98)00187-0